

Josephson φ -junctions based on structures with complex normal/ferromagnet bilayer

S. V. Bakurskiy,^{1,2} N. V. Klenov,¹ T. Yu. Karminskaya,² M. Yu. Kupriyanov,² and A. A. Golubov³

¹*Faculty of Physics, M.V. Lomonosov Moscow State University, 119992 Leninskie Gory, Moscow, Russia*

²*Skobeltsyn Institute of Nuclear Physics, Lomonosov Moscow State University 1(2), Leninskie gory, Moscow 119991, Russian Federation*

³*Faculty of Science and Technology and MESA+ Institute for Nanotechnology,
University of Twente, 7500 AE Enschede, The Netherlands*

(Dated: August 30, 2012)

We demonstrate that Josephson devices with nontrivial phase difference $0 < \varphi_g < \pi$ in the ground state can be realized in structures composed from longitudinally oriented normal metal (N) and ferromagnet (F) films in the weak link region. Oscillatory coupling across F-layer makes the first harmonic in the current-phase relation relatively small, while coupling across N-layer provides negative sign of the second harmonic. To derive quantitative criteria for a φ -junction, we have solved two-dimensional boundary-value problem in the frame of Usadel equations for overlap and ramp geometries of S-NF-S structures. Our numerical estimates show that φ -junctions can be fabricated using up-to-date technology.

PACS numbers: 74.45.+c, 74.50.+r, 74.78.Fk, 85.25.Cp

I. INTRODUCTION

The relation between supercurrent I_S across a Josephson junction and phase difference φ between the phases of the order parameters of superconducting (S) banks is an important characteristic of a Josephson structure^{1,2}. In standard SIS structures with tunnel type of conductivity of a weak link, the current-phase relation (CPR) has the sinusoidal form $I_S(\varphi) = A \sin(\varphi)$. On the other hand, in SNS or SINIS junctions with metallic type of conductivity the smaller the temperature T the larger the deviations from the $\sin(\varphi)$ form¹ and $I_S(\varphi)$ achieves its maximum at $\pi/2 \leq \varphi \leq \pi$. In SIS junctions the amplitude B of second harmonic in CPR, $B \sin(2\varphi)$, is of the second order in transmission coefficient of the tunnel barrier I and therefore is negligibly small for all T . In SNS structures the second CPR harmonic is also small in the vicinity of critical temperature T_C of superconductors, where $A \sim (T_C - T)$. At low temperatures $T \ll T_C$, the coefficients A and B have comparable magnitudes, thus giving rise to qualitative modifications of CPR shape with decrease of T .

It is important to note that in all types of junctions discussed above the ground state is achieved at $\varphi = 0$, since at $\varphi = \pi$ a junction is at nonequilibrium state.

The situation changes in Josephson structures involving ferromagnets as weak link materials. The possibility of the so-called “ π -state” in SFS Josephson junctions (characterized by the negative sign of the critical current I_C) was predicted theoretically and observed experimentally [2-29]. Contrary to traditional Josephson structures, in SFS devices it is possible to have the ground state $\varphi_g = \pi$ (so-called π -junctions), while the $\varphi = 0$ corresponds to an unstable situation. It was proven experimentally^{30,31} that π -junctions can be used as on-chip π -phase shifters or π -batteries for self-biasing various electronic quantum and classical circuits. It was proposed to use self π -biasing to decouple quantum circuits from environment or to replace conventional inductance and strongly reduce the size of an elementary cell³².

In some classical and quantum Josephson circuits it is even more interesting to create on-chip φ -batteries. They are φ -junctions, the structures having phase difference $\varphi_g = \varphi$, ($0 <$

$|\varphi| < \pi$) between superconducting electrodes in the ground state. The φ -states were first predicted by Mints³³ for the case of randomly distributed alternating 0- and π - Josephson junctions along grain boundaries in high T_c cuprates with d-wave order parameter symmetry. It was shown later that φ -junctions can be also realized in the periodic array of 0 and π SFS junctions^{34,35}. It was demonstrated that depending on the length of 0 or π segments in the array, a modulated state with the average phase difference φ_g can be generated if the mismatch length between the segments is small. This φ_g can take any value within the interval $-\pi \leq \varphi_g \leq \pi$. Despite strong constraints on parameter spread of individual segments estimated in³⁶, remarkable progress was recently achieved on realization of φ -junctions in such arrays³⁷.

In general, in order to implement a φ -junction one has use a Josephson junction having non-sinusoidal current-phase relation, which, at least, can be described by a sum of two terms

$$I_S(\varphi) = A \sin(\varphi) + B \sin(2\varphi). \quad (1)$$

Moreover, the following special relationship between the amplitudes of the CPR harmonics, A , and, B , is needed for existence of equilibrium stable state^{38,39}

$$|B| > |A|/2, B < 0. \quad (2)$$

In conventional junctions, the magnitude of A is larger than that of B and the inequalities (2) are difficult to fulfill. However, in SFS junctions in the vicinity of 0 to π transition the amplitude of first harmonic in CPR is close to zero, thus opening an opportunity for making a φ - battery, if B can be made negative. It is well-known that SFS junctions with metallic type of conductivity, as well as SIFS structures^{40,41} with high transparencies of SF interfaces have complex decay length of superconducting correlations induced into F-layer $\xi_H = \xi_1 + i\xi_2$. Unfortunately, the conditions (2) are violated in these types junctions since the $A \sim \exp\{-L/\xi_1\} \cos(L/\xi_2)$, $B \sim -\exp\{-2L/\xi_1\} \cos(2L/\xi_2)$, and for $L = (\pi/2)\xi_2$ corresponding to the first 0- π transition the second harmonic amplitude B is positive.

Quantitative calculations made in the framework of microscopic theory^{42,43} confirm the above qualitative analysis. In

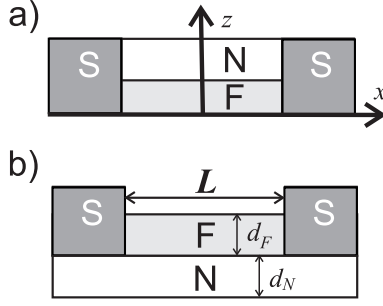


FIG. 1: a) The $S-NF-S$ junction, b) the $SN-FN-NS$ junction.

Ref.^{42,43} it was demonstrated that in SFS sandwiches with either clean or dirty ferromagnetic metal interlayer the transition from 0 to π state is of the first order, that is $B > 0$ at any transition point³.

It was suggested recently in⁴⁴⁻⁴⁹ to fabricate the "current in plane" SFS devices having the weak link region consisting from NF or FNF multilayers with the supercurrent flowing parallel to FN interfaces. In these structures, superconductivity is induced from the S banks into the normal (N) film, while F films serves as a source of spin polarized electrons, which diffuse from F to N layer thus providing an effective exchange field in a weak link. Its strength it can be controlled^{50,51} by transparencies of NF interfaces, as well as by the products of densities of states at the Fermi level, N_F , N_N , and film thicknesses, d_F , d_N . It was shown in⁴⁴⁻⁴⁸ that the reduction of effective exchange energy in a weak link permits to increase the decay length from the scale of the order of ~ 1 nm up to ~ 100 nm. The calculations performed in these papers did not go beyond linear approximation in which the amplitude of the second harmonic in the CPR is small. Therefore, the question of the feasibility of φ -contacts in these structures has not been studied and remains open to date.

The purpose of this paper is to demonstrate that the same "current in plane" devices (see Fig. 1) can be used as effective φ -shifters. The structure of the paper is the following. In Sec.II we present general qualitative discussion of the microscopic mechanisms leading to formation of higher harmonics in the CPR. In Sec.III we formulate quantitative approach in terms of Usadel equations. In Sec.IV the criteria of φ -state existence are derived for ramp-type S-FN-S structure. Section V shows the advantage of the other geometries in order to realize φ -state. Finally in Sec.VI we consider properties of real materials and estimate the possibility to realize φ -states using up-to-date technology.

II. CPR FORMATION MECHANISMS

In this section we shall discuss microscopic processes which contribute to formation of CPR in Josephson junctions. The physical reason leading to the sign reversal of the coefficient B in SFS junctions compared to that in SNS structures can be understood from simple diagram shown in Fig.2 illustrating the mechanisms of supercurrent transfer in double

barrier Josephson junctions.

Consider electron-like quasiparticle e^- propagating across SINIS structure towards the right electrode. This quasiparticle can be reflected either in the Andreev or in the normal channel.

The result of the first process (see Fig.2a) is generation in the weak link region (with an amplitude proportional to $\exp(i\chi_2)$) of the hole h^+ propagating in the opposite direction. Andreev reflection of this hole at the second interface (with an amplitude proportional to $\exp(-i\chi_1)$) results in transfer of a Cooper pair from the left to the right electrode with the rate proportional to the net coefficient of Andreev reflection processes^{52,53} at both SN interfaces, $AR(\varphi) = \alpha(\varphi)\exp(i\varphi)$, $\varphi = (\chi_2 - \chi_1)$. The amplitude, $\alpha(\varphi)$, depends on geometry of a structure and on material parameters. Note that for given values of these parameters $\alpha(\varphi) = \alpha(-\varphi)$, according to the detailed balance relations⁵². Similar considerations show that a quasiparticle e^- moving towards the left electrode generates a Cooper pair propagating from the right to the left interface with the rate proportional to $AR(-\varphi) = \alpha(\varphi)\exp(-i\varphi)$. The difference between two processes described above determines a supercurrent I_S , which is proportional to $\sin(\varphi)$.

The result of the second process is the change (with an amplitude proportional to $\exp(i\chi_2)$) of the e^- propagation direction to the left electrode and nucleation of a Cooper pair and a hole propagating to the right electrode (with an amplitude proportional to $\exp(-i\varphi)$). After normal reflection from the right interface (with an amplitude proportional to $\exp(i\chi_2)$) the hole arrives at the left SN interface and closes this Andreev loop by generating a Cooper pair in the left electrode and an electronic state (with an amplitude proportional to $\exp(-i\chi_1)$). The Cooper pair have to undergo a full reflection at SN interface, thus again a pair is generated moving in the direction opposite to that in the main Andreev loop. The net coefficient of this Andreev reflection process is $BR(\varphi) = \beta(\varphi)\exp(2i\varphi)$. For a quasiparticle e^- moving in the weak link towards the left electrode the same consideration leads to generation of two Cooper pairs moving from the left to the right with the rate proportional to $BR(-\varphi) = \beta(\varphi)\exp(-2i\varphi)$. The difference between these two processes determines a part of supercurrent I_S proportional to $\sin(2\varphi)$.

We have shown that supercurrent components proportional to $\sin(\varphi)$ and $\sin(2\varphi)$ have opposite signs, and the coefficient B in Eq.(1) is negative. This statement is in a full agreement with calculations of the CPR performed in the frame of microscopic theory of superconductivity^{1,2}. It is valid if a supercurrent across a junction does not suppress superconductivity in S electrodes in the vicinity of SN interfaces⁵⁴⁻⁵⁶. In addition, an effective path of the particles in the second process discussed above is two times larger than in the first one. This leads to stronger decay of the second harmonic amplitude B with increasing the distance L .

In SFS junctions the situation becomes more complicated. The exchange field, H , in the weak link removes the spin degeneracy of quasiparticles. As a result, one has to consider four types of Andreev's loops instead of two loops discussed above. One should also take into account the fact that wave function of a quasiparticle propagating through the weak link

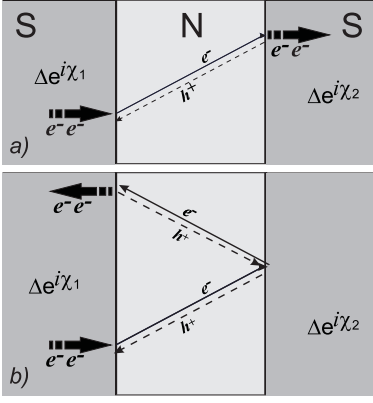


FIG. 2: Diagrams of the processes forming the first (a) and second (b) harmonics of the CPR in the SNS and SFS structures.

acquires an additional phase shift φ_H proportional to the magnitude of the exchange field⁵⁷. The sign of φ_H depends on mutual orientations between magnetization of the ferromagnetic film and the spin of a quasiparticle. Taking into account these phase shifts and repeating arguments similar to given above, one can show that the coefficients A and B in Eq.(1) acquire additional factors $\cos(2\varphi_H)$ and $\cos(4\varphi_H)$, respectively. At the point of "0" - " π " transition the coefficient $A = 0$, that is $\varphi_H = \pi/4$. As a result, $\cos(4\varphi_H)$ provides an additional factor, which changes the sign of the second harmonic amplitude B in SFS structures from negative to positive.

In the present study we will show that contrary to SFS devices with standard geometry, it's possible to realize φ -junctions in the structures shown in Fig. 1. Qualitatively, these structures are superpositions of parallel SNS and SFS-channels, where supercurrent $I_S(\varphi)$ can be decomposed into two parts, $I_N(\varphi)$ and $I_F(\varphi)$, flowing across N and F films, respectively. For $L \ll \xi_N$ and at sufficiently low temperatures $I_N(\varphi)$ has large negative second CPR harmonic B_N . For $L > \xi_1$ supercurrent in the SFS-channel exhibits damped oscillations as a function of L . In this regime the second harmonic of CPR is negligibly small compared to the first one. Large difference between decay lengths of superconducting correlations in N and F-materials allows one to enter the regime when $\xi_1 < L < \xi_N$. In this case the first CPR harmonic $A = A_N + A_F$ can be made small enough due to negative sign of A_F , while the second CPR harmonic $B \approx B_N$ is negative, thus making it possible to fulfill the condition (2). Note that we are considering here the regime of finite interface transparencies, when higher order harmonics decay fast with the harmonic order. Therefore, it is sufficient to consider only the first and the second harmonics of the CPR in all our subsequent discussions.

We show below that the mechanism described above indeed works in the considered S-FN-S junctions, and we estimate corresponding parameter range when φ -states can be realized.

III. MODEL

We consider two types of symmetric multilayered structures shown schematically on Fig.1. The structures consist of a superconducting (S) electrode contacting either the end-wall of a FN bilayer (ramp type junctions) or the surface of F or N films (overlap junction geometry). The FN bilayer consists of ferromagnetic (F) film and normal metal (N) having a thickness d_F , and d_N respectively. We suppose that the conditions of a dirty limit are fulfilled for all metals and that effective electron-phonon coupling constant is zero in F and N films. For simplicity we assume that the parameters γ_{BN} and γ_{BF} which characterize the transparencies of NS and FS interfaces are large enough

$$\gamma_{BN} = \frac{R_{BN} \mathcal{A}_{BN}}{\rho_N \xi_N} \gg \frac{\rho_S \xi_S}{\rho_N \xi_N}, \quad \gamma_{BF} = \frac{R_{BF} \mathcal{A}_{BF}}{\rho_F \xi_F} \gg \frac{\rho_S \xi_S}{\rho_F \xi_F}, \quad (3)$$

in order to neglect suppression of superconductivity in S parts of the junctions. Here R_{BN}, R_{BF} and $\mathcal{A}_{BN}, \mathcal{A}_{BF}$ are the resistances and areas of the SN and SF interfaces, ξ_S, ξ_N and ξ_F are the decay lengths of S, N, F materials and ρ_S, ρ_N and ρ_F are their resistivities.

Under the above conditions the problem of calculation of the supercurrent in the structures reduces to solution of the set of Usadel equations^{3,4,58}

$$\frac{\xi^2}{G_\omega} \partial [G_\omega^2 \partial \Phi_\omega] - \frac{\tilde{\omega}}{\pi T_C} \Phi_\omega = 0, \quad G_\omega = \frac{\tilde{\omega}}{\sqrt{\tilde{\omega}^2 + \Phi_\omega \Phi_\omega^*}}, \quad (4)$$

where Φ_ω and G_ω are Usadel Green's functions in Φ parametrization. They are $\Phi_{\omega,N}$ and $G_{\omega,N}$ or $\Phi_{\omega,F}$ and $G_{\omega,F}$ in N and F films correspondingly, $\omega = \pi T(2m+1)$ are Matsubara frequencies ($m=0,1,2,\dots$), $\tilde{\omega} = \omega + iH$, H , is exchange field of ferromagnetic material, $\xi^2 = \xi_{N,F}^2 = D_{N,F}/2\pi T_C$ for N and F layers respectively, $D_{N,F}$ are diffusion coefficients, $\partial = (\partial/\partial x, \partial/\partial z)$ is 2D gradient operator. To write equations (4), we have chosen the z and x axis in the directions, respectively, perpendicular and parallel to the plane of N film and we have set the origin in the middle of structure at the free interface of F-film (see Fig.1).

The supercurrent $I_S(\varphi)$ can be calculated by integrating the standard expressions for the current density $j_{N,F}(\varphi, z)$ over the junction cross-section:

$$\frac{2e j_{N,F}(\varphi, z)}{\pi T} = \sum_{\omega=-\infty}^{\infty} \frac{i G_\omega^2}{\rho_{N,F} \tilde{\omega}_{N,F}^2} \left[\Phi_\omega \frac{\partial \Phi_\omega^*}{\partial x} - \Phi_\omega^* \frac{\partial \Phi_\omega}{\partial x} \right], \quad (5)$$

$$I_S(\varphi) = W \int_0^{d_F} j_F(\varphi, z) dz + W \int_{d_F}^{d_F+d_N} j_N(\varphi, z) dz,$$

where W is the width of the junctions, which is supposed to be small compared to Josephson penetration depth. It is convenient to perform the integration in (5) in F and N layers separately along the line located at $x = 0$, where z -component of supercurrent density vanishes by symmetry.

Eq.(4) must be supplemented by the boundary conditions⁵⁹. Since these conditions link the Usadel Green's functions corresponding to the same Matsubara frequency ω , we may simplify the notations by omitting the subscript ω . At the NF

interface the boundary conditions have the form:

$$\begin{aligned}\gamma_{BFN}\xi_F\frac{\partial\Phi_F}{\partial z} &= -\frac{G_N}{G_F}\left(\Phi_F - \frac{\tilde{\omega}}{\omega}\Phi_N\right), \\ \gamma_{BNF}\xi_N\frac{\partial\Phi_N}{\partial z} &= \frac{G_F}{G_N}\left(\Phi_N - \frac{\omega}{\tilde{\omega}}\Phi_F\right),\end{aligned}\quad (6)$$

$$\gamma_{BFN} = \frac{R_{BFN}\mathcal{A}_{BFN}}{\rho_F\xi_F} = \gamma_{BNF}\frac{\rho_F\xi_F}{\rho_N\xi_N},$$

where R_{BFN} and \mathcal{A}_{BFN} are the resistance and area of the NF interface.

The conditions at free interfaces are

$$\frac{\partial\Phi_N}{\partial n} = 0, \quad \frac{\partial\Phi_F}{\partial n} = 0. \quad (7)$$

The partial derivatives in (7) are taken in the direction normal to the boundary, so that n can be either z or x depending on the particular geometry of the structure.

In writing the boundary conditions at the interface with a superconductor, we must take into account the fact that in our model we have ignored the suppression of superconductivity in electrodes, so that in superconductor

$$\Phi_S(\pm L/2) = \Delta \exp(\pm i\varphi/2), \quad G_S = \frac{\omega}{\sqrt{\omega^2 + \Delta^2}}, \quad (8)$$

where Δ is magnitude of the order parameter in S banks. Therefore for NS and FS interfaces we may write:

$$\gamma_{BN}\xi_N\frac{\partial\Phi_N}{\partial n} = \frac{G_S}{G_N}(\Phi_N - \Phi_S(\pm L/2)), \quad (9a)$$

$$\gamma_{BF}\xi_F\frac{\partial\Phi_F}{\partial n} = \frac{G_S}{G_F}\left(\Phi_F - \frac{\tilde{\omega}}{\omega}\Phi_S(\pm L/2)\right). \quad (9b)$$

As in Eq. (7), n in Eqs. (9a), (9b) is a normal vector directed into material marked at derivative.

For the structure presented in Fig.1a, the boundary-value problem (4) - (9b) was solved analytically in the linear approximation^{47,48}, i.e. under conditions

$$G_N \equiv \text{sgn}(\omega), \quad G_F \equiv \text{sgn}(\omega). \quad (10)$$

In the present study we will go beyond linear approximation where qualitatively new effects are found.

IV. RAMP-TYPE GEOMETRY

The ramp type Josephson junction has simplest geometry among the structures shown in Fig.1. It consists of the NF bilayer, laterally connected with superconducting electrodes (see Fig.1a).

In general, there are three characteristic decay lengths in the considered structure^{44,47,68}. They are ξ_N , $\xi_H = \xi_1 + i\xi_2$, and $\xi = \xi_1 + i\xi_2$. The first two lengths determine the decay and oscillations of superconducting correlations far from FN interface, while the last one describes their behavior in its vicinity. Similar length scale ξ occurs in a vicinity of a domain

wall⁶⁰⁻⁶⁸. In the latter, exchange field is averaged out for antiparallel directions of magnetizations, and the decay length of superconducting correlations becomes close to ξ_N . At FN interface, the flow of spin-polarized electrons from F to N metal and reverse flow of unpolarized electrons from N to F suppresses the exchange field in its vicinity to a value smaller than that in a bulk ferromagnetic material thus providing the existence of ξ . Under certain set of parameters⁴⁴ these lengths, ξ_1 , and, ξ_2 , can become comparable to ξ_N , which is typically much larger than ξ_1 and ξ_2 , which are equal to $\xi_F\sqrt{\pi T_C/H}$ for $H \gg \pi T_C$.

The existence of three decay lengths, ξ_N , ξ , and ξ_H , should lead to appearance of three contributions to total supercurrent, I_N , I_{FN} and I_F , respectively. The main contribution to I_N component comes from a part of the supercurrent uniformly distributed in a normal film. In accordance with the qualitative analysis carried out in Section II, it is the only current component which provides a negative value of the amplitude of the second harmonic B in the current-phase relation. The smaller the distance between electrodes L , the larger this contribution. To realize a φ -contact, one must compensate for the amplitude of the first harmonic, A , in a total current to a value that satisfies the requirement (2). Contribution to A from I_N also increases with decreasing L . Obviously, it's difficult to suppress the coefficient A due to the I_{FN} contribution only, since I_{FN} flows through thin near-boundary layer. Therefore, strong reduction of A required to satisfy the inequality (2) can only be achieved as a result of compensation of the currents I_N and I_F flowing in opposite directions in N and F films far from FN interface. Note that the oscillatory nature of the $I_F(L)$ dependence allows to satisfy requirement (2) in a certain range of L . The role of I_{FN} in a balance between I_N and I_F can be understood by solving the boundary value problem (4) - (9b) which admits an analytic solution in some limiting cases.

A. Limit of small L .

Solution of the boundary-value problem (4)-(9b) can be simplified in the limit of small distance between superconducting electrodes

$$L \ll \min\{\xi_1, \xi_N\}. \quad (11)$$

In this case one can neglect non-gradient terms in (4) and obtain that contributions to the total current resulting from the redistribution of currents near the FN interface cancel each other leading to $I_{FN} = 0$ (see Appendix A for the details). As a result, the total current $I_S(\varphi)$ is a sum of two terms only

$$I_S(\varphi) = I_N(\varphi) + I_F(\varphi),$$

$$\frac{2eI_N(\varphi)}{\pi T W d_N} = \frac{1}{\gamma_{BN}\xi_N\rho_N} \sum_{\omega=-\infty}^{\infty} \frac{\Delta^2 G_N G_S \sin(\varphi)}{\omega^2}, \quad (12)$$

$$\frac{2eI_F(\varphi)}{\pi T W d_F} = \frac{1}{\gamma_{BF}\xi_F\rho_F} \sum_{\omega=-\infty}^{\infty} \frac{\Delta^2 G_N G_S \sin(\varphi)}{\omega^2}, \quad (13)$$

where $G_N = \frac{\omega}{\sqrt{\omega^2 + \Delta^2 \cos^2(\frac{\varphi}{2})}}$. The currents $I_N(\varphi)$ and $I_F(\varphi)$ flow independently across F and N parts of the weak link. The $I_{N,F}(\varphi)$ dependencies coincide with those calculated previously for double-barrier junctions⁵⁹ in the case when L lies within the interval defined by the inequalities (11).

It follows from (12), (13) that in the considered limit neither the presence of a sharp FN boundary in the weak link region, nor strong difference in transparencies of SN and SF interfaces lead to intermixing of the supercurrents flowing in the F and N channels. It is also seen that amplitude of the first harmonic of $I_F(\varphi)$ current component is always positive and the requirement (2) can not be achieved.

B. Limit of intermediate L .

For intermediate values of spacing between the S electrodes

$$\xi_1 \ll L \ll \xi_N \quad (14)$$

and for the values of suppression parameters at SN and SF interfaces satisfying the conditions (3), the boundary problem (4)-(9b) can be solved analytically for sufficiently large magnitude of suppression parameter γ_{BFN} . It is shown in Appendix B that under these restrictions in the first approximation we can neglect the suppression of superconductivity in the N film due to proximity with the F layer and find that

$$\Phi_N = \Delta \cos\left(\frac{\varphi}{2}\right) + i \frac{\Delta G_S \sin(\frac{\varphi}{2})}{\gamma_{BN} G_N} \frac{x}{\xi_N}, \quad G_N = \frac{\omega}{\sqrt{\omega^2 + \Delta^2 \cos^2(\frac{\varphi}{2})}}, \quad (15)$$

while spatial distribution of $\Phi_F(x, z)$ includes three terms: the first two describe the influence of the N film, while the last one has the form well known for SFS junctions^{2,3,4}.

Substitution of these solutions into expression for the supercurrent (5) leads to $I_S(\varphi)$ dependence consisting of three terms

$$I_S(\varphi) = I_N(\varphi) + I_F(\varphi) + I_{FN}(\varphi). \quad (16)$$

Here $I_N(\varphi)$ is the supercurrent across the N layer. In the considered approximation $I_N(\varphi)$ is given by the expression (12). The second term in (16) equals to supercurrent across SFS double barrier structure in the limit of small transparencies of SF interfaces^{69,70}

$$\frac{2eI_F(\varphi)}{\pi T W d_F} = \frac{\Delta^2 \sin(\varphi)}{\gamma_{BF}^2 \xi_F \rho_F} \sum_{\omega=-\infty}^{\infty} \frac{G_S^2}{\omega^2 \sqrt{\tilde{\Omega}} \sinh(2q_L)}, \quad (17)$$

where $q_L = L\sqrt{\tilde{\Omega}}/2\xi_F$, $\tilde{\Omega} = |\Omega| + iH \operatorname{sgn}(\Omega)/\pi T_C$, $\Omega = \omega/\pi T_C$.

The last contribution is shown in B to contain three components

$$I_{FN}(\varphi) = I_{FN1}(\varphi) + I_{FN2}(\varphi) + I_{FN3}(\varphi). \quad (18)$$

with additional smallness parameters γ_{BFN}^{-1} and $\gamma_{BFN}^{-1} \xi_F/\xi_N$ compared to the current $I_F(\varphi)$ given by Eq.(17). Nevertheless, these currents should be taken into account in the analysis because they decay significantly slower than $I_F(\varphi)$ with increasing L .

C. φ -state existence

The conditions for the implementation of a φ -contact are the better, the larger the relative amplitude of the second harmonic which increases at low temperatures. Therefore, low temperature regime is most favorable for a φ -state. In the limit $T \ll T_C$ we can go from summation to integration over ω in (12), (17), (B15)- (B17). From (12) we have

$$\frac{2eI_N(\varphi)}{W d_N} = \frac{\Delta}{\gamma_{BN} \xi_N \rho_N} K(\sin \frac{\varphi}{2}) \sin(\varphi), \quad (19)$$

where $K(x)$ is the complete elliptic integral of the first kind. Expanding expression (19) in the Fourier series it is easy to obtain

$$A_N = Q_0 \frac{8}{\pi} \int_0^1 x^2 \sqrt{1-x^2} K(x) dx = \Upsilon_A Q_0, \quad (20)$$

$$B_N = 2A_N - \frac{32}{\pi} Q_0 \int_0^1 x^4 \sqrt{1-x^2} K(x) dx = \Upsilon_B Q_0, \quad (21)$$

where $Q_0 = \Delta W d_N / e \gamma_{BN} \xi_N \rho_N$, A_N , B_N are the first and the second harmonic amplitudes of $I_N(\varphi)$,

$$\begin{aligned} \Upsilon_A &= \frac{2\pi^2}{\Gamma^2(-\frac{1}{4})\Gamma^2(\frac{7}{4})} \simeq 0.973, \\ \Upsilon_B &= 2\Upsilon_A - \frac{\pi}{2} {}_3F_2\left(\frac{1}{2}, \frac{1}{2}, \frac{5}{2}; 1, 4; 1\right) \simeq -0.146, \end{aligned}$$

where $\Gamma(z)$ is Gamma-function and ${}_pF_q$ is generalized hypergeometric function.

Evaluation of the sums in (17), (B15)- (B17) can be done for $H \gg \pi T_C$ and $T \ll T_C$ resulting in $I_F(\varphi) = A_F \sin(\varphi)$ with

$$A_F = P_0 \frac{2}{\sqrt{h}} \exp(-\kappa L) \cos\left(\kappa L + \frac{\pi}{4}\right), \quad (22)$$

$\kappa = \sqrt{h}/\sqrt{2}\xi_F$, $h = H/\pi T_C$ and $P_0 = \Delta W d_F / e \gamma_{BF}^2 \xi_F \rho_F$. Substitution of (20), (21) into the inequalities (2) gives φ -state requirements for ramp-type structure

$$\left| \Upsilon_A + \frac{1}{\varepsilon} \Psi(L) \right| < 2|\Upsilon_B|, \quad \varepsilon = \frac{\sqrt{h} \gamma_{BF}^2}{2\gamma_{BN}} \frac{d_N \xi_F \rho_F}{d_F \xi_N \rho_N}, \quad (23)$$

$$\Psi(L) = \exp(-\kappa L) \cos\left(\kappa L + \frac{\pi}{4}\right).$$

This expression gives the limitation on geometrical and materials parameters of the considered structures providing the existence of φ -junction. Function $\Psi(L)$ has the first minimum at $\kappa L = \pi/2$, $\Psi(\pi/2\kappa) \approx -0.147$. For large values of ε inequality (23) can not be fulfilled at any length L . Thus solutions exist only in the area with upper limit

$$\varepsilon < \frac{-\Psi(\pi/2\kappa)}{\Upsilon_A - 2|\Upsilon_B|} \approx 0.216. \quad (24)$$

At $\varepsilon \approx 0.216$ the left hand side of inequality (23) equals to its right hand part providing the nucleation of an interval of κL in which we can expect the formation of a φ -contact. This interval increases with decrease of ε and achieves its maximum length

$$1.00 \lesssim \kappa L \lesssim 2.52, \quad (25)$$

at $\varepsilon = \frac{-\Psi(\pi/2\kappa)}{\Upsilon_A + 2|\Upsilon_B|} \approx 0.116$. It is necessary to note that at $\varepsilon = -\Psi(\pi/2\kappa)/\Upsilon_A \approx 0.151$ there is a transformation of the left hand side local minimum in (23), which occurs at $\kappa L = \pi/2$, into local maximum; so that at $\varepsilon \approx 0.116$ the both sides of (23) become equal to each other, and the interval (25) of φ -junction existence subdivides into two parts. With a further decrease of ε these parts are transformed into narrow bands, which are localized in the vicinity of the $0 - \pi$ transition point ($A_N + A_F = 0$); they take place at $\kappa L = \pi/4$ and $\kappa L = 5\pi/4$. The width of the bands decreases with decrease of ε .

Thus, our analysis has shown that for

$$0.12 \lesssim \varepsilon \lesssim 0.2 \quad (26)$$

we can expect the formation of φ -junction in a sufficiently wide range of distances ΔL between the electrodes determined by (23). Now we will take into the account the impact of the interface term $I_{FN}(\varphi)$. In the considered approximations, it follows from (B15)- (B17) that

$$I_{FN1}(\varphi) = \frac{2U_0\xi_F \exp(-\frac{\kappa L}{2}) \cos(\frac{\kappa L}{2} - \frac{\pi}{4})}{\gamma_{BF}\gamma_{BN}\xi_N h^{3/2}} \sin(\varphi), \quad (27)$$

$$I_{FN2}(\varphi) = -\frac{\sqrt{2}U_0\xi_F}{4h^{3/2}\gamma_{BN}\gamma_{BFN}\xi_N} \sin(\varphi) K(\sin \frac{\varphi}{2}), \quad (28)$$

$$I_{FN3}(\varphi) = -\frac{2U_0 \exp(-\frac{\kappa L}{2}) \sin(\frac{\kappa L}{2})}{h\gamma_{BF}} \sin(\varphi) K(\sin \frac{\varphi}{2}), \quad (29)$$

where $U_0 = \Delta W/e\gamma_{BFN}\rho_F$. In the range of distances between the electrodes $\pi/4 < \kappa L < 5\pi/4$ currents $I_{FN2}(\varphi)$ and $I_{FN3}(\varphi)$ are negative. These contributions have the same form of CPR as it is for the $I_N(\varphi)$ term, and due to negative sign suppress the magnitude of supercurrent across the junction thus making the inequality (23) easier to perform. The requirement $B < 0$ imposes additional restriction on the value of the suppression parameter γ_{BFN}

$$\gamma_{BFN} > \frac{\rho_N \xi_N}{h d_N \rho_F} \left(\frac{\xi_F}{\xi_N \gamma_{BFN} h^{1/2}} + \frac{\gamma_{BN}}{\gamma_{BF}} \right). \quad (30)$$

In derivation of this inequality we have used the fact that in the range of distances between the electrodes $\pi/4 < \kappa L < 5\pi/4$ depending on κL factor in (29) is of the order of unity. It follows from (30) that for a fixed value of γ_{BFN} domain of φ -junction existence extends with increase of thickness of

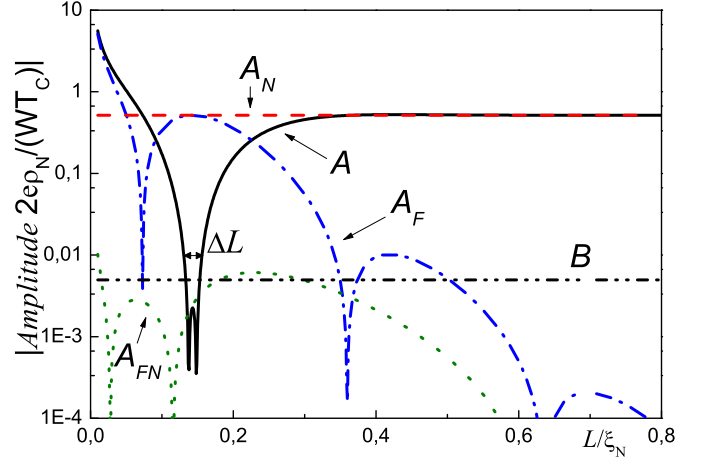


FIG. 3: Analytically derived amplitudes A and B in the CPR of ramp S-NF-S structure ($d_N = 0.1\xi_N$, $d_F = 0.65\xi_N$) and their components A_N , A_F , A_{FN} versus electrode spacing L at $T = 0.7T_C$. Also enhanced interval of φ -state, ΔL , is marked.

normal films d_N and this domain disappears if d_N becomes smaller than the critical value, d_{NC} ,

$$d_{NC} = \frac{\rho_N \xi_N}{h \rho_F \gamma_{BFN}} \left(\frac{\xi_F}{\xi_N \gamma_{BFN} h^{1/2}} + \frac{\gamma_{BN}}{\gamma_{BF}} \right). \quad (31)$$

The existence of the critical thickness d_{NC} follows from the fact that the amplitude B in I_N is proportional to d_N , while in I_{FN} term the parameter B is independent on d_N . The sign of $I_{FN1}(\varphi)$ is positive for $\pi/4 < \kappa L < 3\pi/4$ and negative for $3\pi/4 < \kappa L < 5\pi/4$ thus providing an advantage for a φ -junction realization for the lengths which belong to the second interval.

Figure 3 illustrates our analysis. The solid line in Fig.3 is the modulus of the amplitude of the first harmonic in CPR as a function of distance L between S electrodes. It is the result of summation of the two contributions following from Eqs. (17) (dash-dotted line) and (12) (dashed line). The dash-dot-dotted line in Fig 3 is the amplitude of the second harmonic of the CPR following from (12). The dotted line is $I_{FN}(L)$ calculated from (18), (B15)- (B17). All calculations have been done for a set of parameters $d_N = 0.1\xi_N$, $d_F = 0.65\xi_N$, $\gamma_{BN} = 0.1$, $\gamma_{BF} = 1$, $\gamma_{BFN} = 10$, $\xi_F = 0.1\xi_N$, $\rho_N = \rho_F$, $T = 0.7T_C$, $H = 10T_C$. These parameters are close to those in real experimental situation. All the amplitudes were normalized on factor $(2e\rho_N/(WT_C))^{-1}$. It is evident that there is an interval of L , for which the currents in N and F layers flow in opposite directions. As a result of the addition of these currents the points of $0 - \pi$ transitions start to be closer to each other. It is seen that in the entire region between these points, the inequality (2) is fulfilled. This is exactly the L -interval, inside which a φ -junction can be realized. It is also seen that contribution of I_{FN} part into the full current is small and in accordance with our analysis does not play a noticeable role.

The boundary problem (4)-(9b) has been solved numerically for the same set of junction parameters except d_F . The results of calculations for $d_F = 1.06\xi_N$ and $d_F = 1.4\xi_N$ are

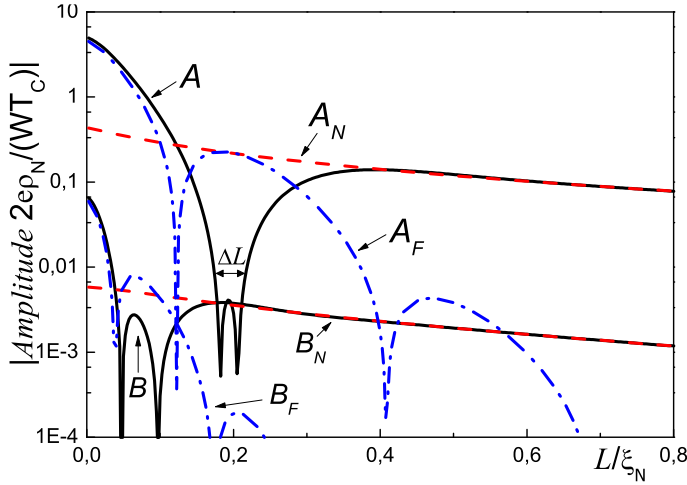


FIG. 4: Numerically calculated amplitudes A and B in the CPR of ramp S-NF-S structure ($d_N = 0.1\xi_N$, $d_F = 1.06\xi_N$) and their components A_N , A_F , B_N , B_F versus electrode spacing L at $T = 0.7T_C$. In correspondence with Fig.3 parameters are chosen to form enhanced φ -state interval marked by " ΔL ".

shown in Fig.4 and Fig.5. The solid lines in Fig.4 are the modulus of the amplitudes of the first, A , and the second, B , harmonic of CPR as a function of distance L between S electrodes. The dashed and dash-dotted lines demonstrate the contributions to these amplitudes from the currents flowing in N and F films, respectively. All the amplitudes were normalized on the same factor $(2ep_N/(WT_C))^{-1}$. It is seen that the main difference between analytical solutions presented in Fig.3 and the curves calculated numerically are located in region of small L . It is also seen that amplitudes of first and second harmonics of the part of the current flowing in the N film slightly decay with L increase. The points of $0 - \pi$ transition of the first harmonic amplitude of the part of the current flow-

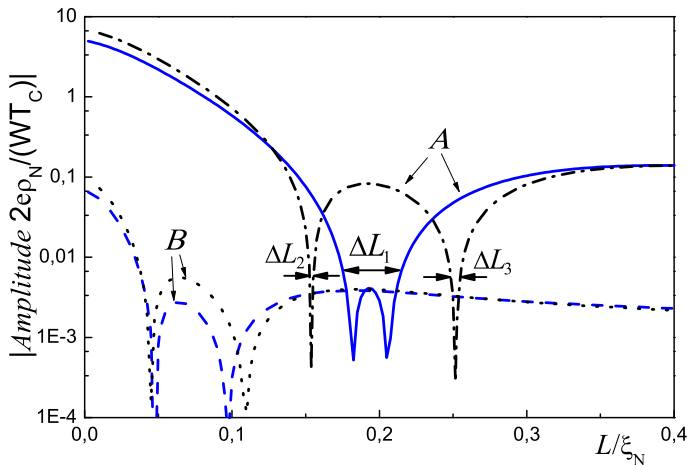


FIG. 5: Numerically calculated CPR amplitudes A and B versus electrode spacing L for S-FN-S structures with $d_F = 1.06\xi_N$ (solid and dashed lines respectively) and $d_F = 1.4\xi_N$ (dash-dotted and dotted lines). It is clear that enhanced φ -interval ΔL_1 formed in the first case is much larger than pair of ordinary φ -intervals ΔL_2 and ΔL_3 in the second one.

ing in the F layer is slightly shifted to the right, toward larger L . It is also seen that the amplitude of the second harmonic, B_F , in the interval of interest in the vicinity of $L \approx 0.2\xi_N$ is negligibly small compared to the magnitude of, B_N . As a result, the shape of $A(L)$ curves in Fig.3 and Fig.4 is nearly the same, with a little bit larger interval of φ -junction existence for the curve calculated numerically.

Figure 5 demonstrates the same $A(L)$ and $B(L)$ dependencies as in Fig.4 (solid and dashed lines) together with $A(L)$ and $B(L)$ curves calculated for $d_F = 1.4\xi_N$ (dash-dotted and dotted lines). It is clearly seen that for larger d_F we get out of the interval (26) and instead of relatively large zone ΔL_1 may have φ -junction in two very narrow intervals ΔL_2 and ΔL_3 located in the vicinity of $0 - \pi$ transitions of the first harmonic amplitude A .

V. RAMP TYPE OVERLAP (RTO) JUNCTIONS

Conditions for the existence of φ -junction (25), (26) can be improved by slight modifications of contact geometry, namely, by using a combination of ramp and overlap configurations, as it is shown in Fig.1b. Fig.6 demonstrates numerically calculated spatial distribution of supercurrent in RTO φ -junction at Josephson phase $\varphi = \pi/2$. The current density is presented by darkness and the arrows give flows directions. The relative smallness of the first harmonics amplitude is provided by opposite currents in N and F films. The main feature of the ramp-overlap geometry is seen to be specific current distribution in the normal layer leading to another CPR shape with dependence on thickness d_N . Further, the current I_N should saturate as a function of d_N , since normal film regions located at distances larger than ξ_N from SN interface are practically excluded from the process of supercurrent transfer due to exponential decay of proximity-induced superconducting correlations⁷¹. The specific geometry of the RTO structures makes theoretical analysis of the processes more complex than in ramp contact. Nevertheless, it is possible to find analytical expressions for supercurrent in these structures and to show that the range of parameters providing the existence of φ -state is broader than in the ramp type configuration.

To prove this statement, we consider the RTO structure in most practical case of thin N film

$$d_N \ll \xi_N \quad (32)$$

and sufficiently large γ_{BFN} providing negligibly small suppression of superconductivity in N film due to proximity with F layer. We will assume additionally that electrode spacing L is also small

$$L \ll \xi_N, \quad (33)$$

in order to have nonsinusoidal CPR. Under these conditions we can at the first step consider the Josephson effect in overlap SN-N-NS structure. Then, at the second step we will use the obtained solutions to calculate supercurrent flowing across the F part of the RTO structure. The details of calculations are

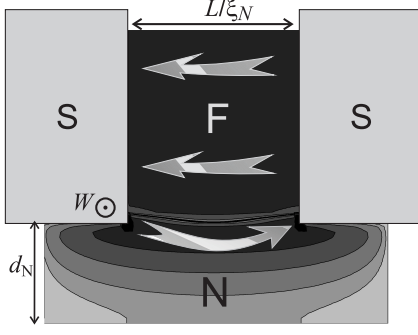


FIG. 6: Current distribution along RTO-type SN-FN-NS structure at $L = 0.63\xi_N$, $d_N = \xi_N$, $d_F = 2\xi_N$ and $T = 0.7T_C$. The intensity of gray color shows current density in direction indicated by arrows.

summarized in Appendices C and D. They give that the super-current

$$I_S(\varphi) = I_N(\varphi) + I_F(\varphi) + I_{FN}(\varphi) \quad (34)$$

consists of three components. Expression for the part of current flowing across N film has the form

$$\frac{2eI_N(\varphi)}{\pi TWd_N} = \frac{2}{\rho_N \xi_N \sqrt{\gamma_{BM}}} \sum_{\omega=-\infty}^{\infty} \frac{r^2 \delta^2 \sin \varphi \sqrt{(\Omega \gamma_{BM} + G_S)}}{\sqrt{2\Omega \mu^2 (\sqrt{\Omega^2 + r^2 \delta^2} + \mu)}}, \quad (35)$$

where $r = G_S/(\Omega \gamma_{BM} + G_S)$, $\gamma_{BM} = \gamma_{BN} d_N / \xi_N$ and $\mu = \sqrt{\Omega^2 + r^2 \delta^2 \cos^2(\varphi/2)}$, $\delta = \Delta / \pi T_C$.

The $I_F(\varphi)$ term in (34) is the current through one dimensional double barrier SFS structure defined by Eq. (17), while $I_{FN}(\varphi)$ is FN-interface term shown in D. We provide sufficient smallness and neglect it in the following estimations.

As we discussed above, the larger the relative amplitude of the second harmonic (or the lower the temperature of a junction compare to T_C), the better the conditions for the implementation of a φ -contact. In the limit $T \ll T_C$ we can transform from summation to integration over ω in (35) and calcu-

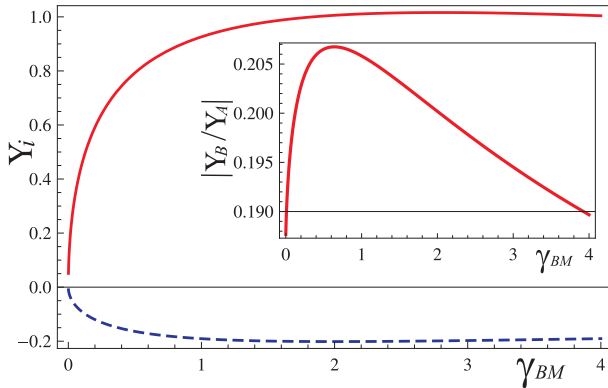


FIG. 7: The amplitudes of the first harmonic Y_A (solid line) and the second one Y_B (dashed line) normalized on $2W\Delta/e\rho_N\gamma_{BN}$ versus reduced thickness γ_{BM} . Inset shows the ratio of harmonics $|Y_B/Y_A|$ versus γ_{BM} .

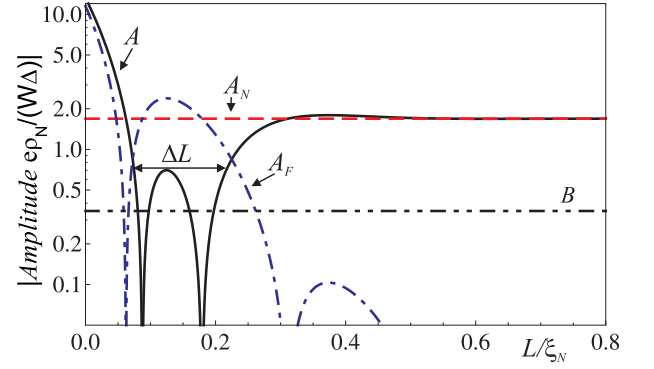


FIG. 8: The amplitudes of CPR harmonics A , A_N , A_F , B versus electrode spacing L for RTO structure at $T \ll T_C$, $\gamma_{BM} = 0.64$ and $\varepsilon = 0.123$. The mark " ΔL " shows enhanced φ -state interval.

late numerically the dependence of amplitudes A and B

$$A_N = \frac{2W\Delta}{e\rho_N\gamma_{BN}} Y_A, \quad (36)$$

$$B_N = \frac{2W\Delta}{e\rho_N\gamma_{BN}} Y_B \quad (37)$$

on suppression parameter γ_{BM} . The calculated dependencies of functions $Y_A(\gamma_{BM})$ and $|Y_B|(\gamma_{BM})$ are presented in Fig.7. It is seen that both Y_A and $|Y_B|$ increase with increasing of γ_{BM} and saturate at $\gamma_{BM} \approx 1$. Inset in Fig.7 shows the ratio of the harmonics $|Y_B/Y_A|$ as a function of γ_{BM} . It achieves maximum at $\gamma_{BM} \approx 0.64$, thus it determines the optimal values of normalized amplitudes of the first $Y_A \approx 0.844$ and the second $Y_B \approx -0.175$ harmonics of the current flowing in the N layer. It is seen from the inset in Fig.7, that the ratio $|Y_B/Y_A|$ is slowly decreasing function of γ_{BM} . Therefore, the estimates given below for $\gamma_{BM} = 0.64$ are applicable in a wide parameter range $0.5 \leq \gamma_{BM} \leq 10$.

Taking into account these values, we can write down the condition of φ -state existence similar to (23)

$$\left| Y_A + \frac{1}{\varepsilon} \Psi(L) \right| \leq 2|Y_B|, \quad \varepsilon = \frac{\sqrt{\hbar} \gamma_{BF}^2}{\gamma_{BN}} \frac{\xi_F \rho_F}{d_F \rho_N}, \quad (38)$$

$$\Psi(L) = \exp(-\kappa L) \cos\left(\kappa L + \frac{\pi}{4}\right),$$

with slightly modified dimensionless parameter ε . The wide region of φ -state still exists if ε is within the interval

$$0.123 \lesssim \varepsilon \lesssim 0.298 \quad (39)$$

for κL that satisfies the condition (38). As follows from (38), interval of κL product gains its maximum length

$$0.94 \lesssim \kappa L \lesssim 2.72, \quad (40)$$

at $\varepsilon = 0.123$. It is seen that these intervals are slightly larger than those given by (25) for the ramp type geometry.

Fig.8 shows the interval of φ -state existence, ΔL , in the ideal case of $T \ll T_C$, $\gamma_{BM} = 0.64$ and $\varepsilon = 0.123$. The corresponding set of parameters $d_N = 0.64\xi_N$, $d_F = 1.45\xi_N$, $\gamma_{BN} = 1$, $\gamma_{BF} = 1$, $\xi_F = 0.1\xi_N$, $\rho_N = \rho_F$, $H = 10T_C$ was substituted in (17), (35). The solid line is a modulus of the first harmonic amplitude, A , its normal, A_N , and ferromagnetic, A_F , parts are presented by dashed and dash-dotted lines respectively. Finally, the second harmonic amplitude is shown as dash-dot-dotted line. It's clear that $|A|$ is relatively small in the wide region ΔL and reaches the value of $|2B|$ only at local maximum. The increased width of ΔL (see Eqs. (29),(49)) is provided by geometric attributes of RTO type structure.

Let us illustrate the range of nontrivial ground phase φ_g existence in the structure described in Fig.8. The total supercurrent I_S is shown on Fig.9 as a function of Josephson phase φ and electrode spacing L . It means that each L -section of this 3D graph is CPR. Solid lines mark the ground state phases at each L . In the range of small and large spacing L ground phase is located at $\varphi_g = 0$. However, in the ΔL -interval CPR becomes significantly nonsinusoidal and demands ground phase φ_g to split and go to π from both sides; then π -state is realized at $\kappa L = \pi/2$. Clearly, for $\varepsilon \gtrsim 0.123$ the value $\varphi_g = \pi$ can not be reached (see Fig.9a), while in the case of $\varepsilon \lesssim 0.123$ the prolonged π -state region is formed (see Fig.9c).

VI. DISCUSSION

We have shown that stable φ -state can be realized in S-NF-S structures with longitudinally oriented NF-bilayers (though φ -state can not be achieved in conventional SNS and SFS structures). We have discussed the conditions for realization of φ -state in ramp-type S-NF-S and RTO-type SN-FN-NS geometries.

Let us discuss most favorable conditions for experimental realization of φ -junction. We suggest to use Copper as a normal film ($\xi_N \approx 100 \text{ nm}$ and $\rho = 5 * 10^{-8} \Omega m$) and strongly diluted ferromagnet like FePd or CuNi alloy ($\xi_F \approx 10 \text{ nm}$, $H \approx 10T_C$) as the F-layer. We chose Nb ($T_C \approx 9K$) as a superconducting electrode material since it is commonly used in superconducting circuits applications. We also propose to use sufficiently thick normal layer, above the saturation threshold, when N-layer thickness have almost no effect. After substitution of relevant values into (39) and (40) we arrived at a fairly broad geometrical margins, within which there is a possibility for implementation of φ -junctions

$$\begin{aligned} d_N &\gtrsim 50 \text{ nm}, \\ 60 \text{ nm} &\lesssim d_F \lesssim 150 \text{ nm}, \\ 7 \text{ nm} &\lesssim L \lesssim 22 \text{ nm}. \end{aligned} \quad (41)$$

Finally, the last out-of-plane geometrical scale is set as $W = 140 \text{ nm}$. This value maximizes current and conserves the scale of structure in a range of 100 nm . The magnitude of critical supercurrent in the φ -state is determined by the second harmonic amplitude B

$$I_C \sim B_N = \frac{2W\Delta}{e\rho_N\gamma_{BN}}\Upsilon_B \approx 1 \text{ mA}. \quad (42)$$

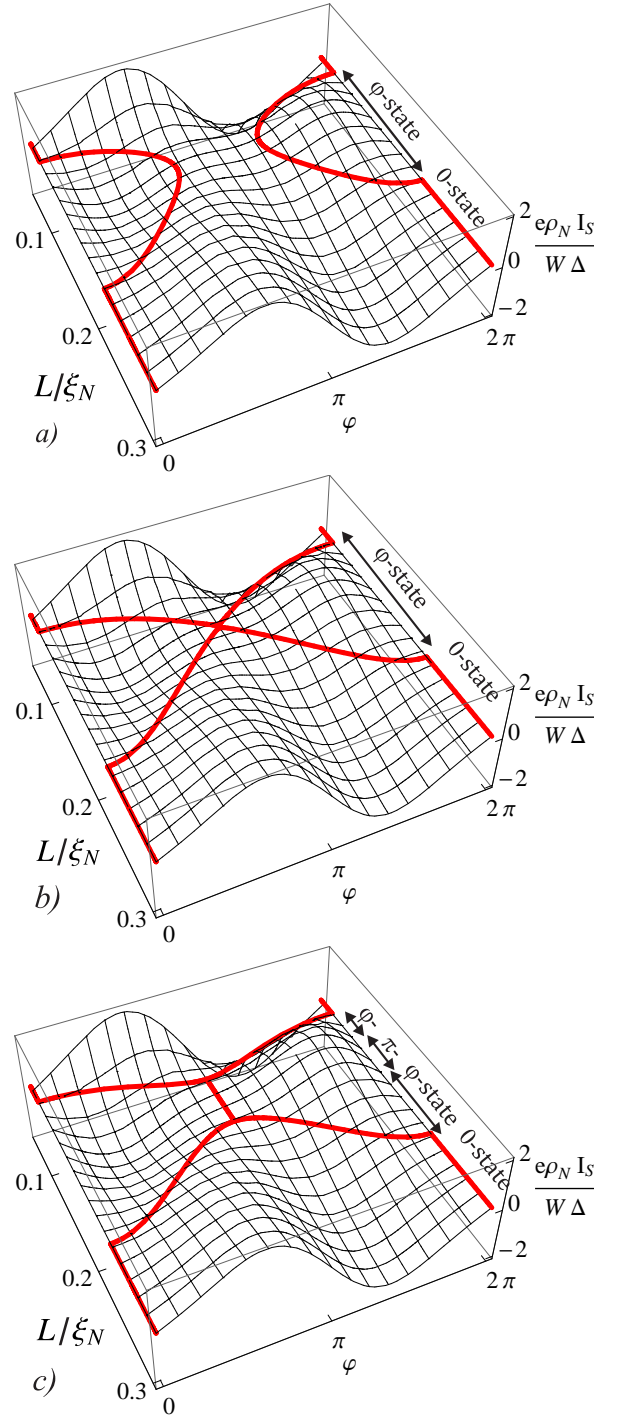


FIG. 9: The full current I_S versus Josephson phase φ and electrode spacing L for RTO structure at $T \ll T_C$, $\gamma_{BM} = 0.64$ and at different F-layer thickness parameters a) $\varepsilon = 0.137$, b) $\varepsilon = 0.123$, c) $\varepsilon = 0.111$. The lines mark the ground states phase φ_g .

The spreads of geometrical scales as well as the magnitude of critical current are large enough to be realized experimentally.

By creating φ -state in a Josephson junction one can fix certain value of ground phase φ_g . Temperature variation slightly shifts the interval of relevant $0-\pi$ transition and permits one

to tune the desired ground state phase. Furthermore, sensitivity of the ground state to an electron distribution function permits φ -junctions to be applied as small-scale self-biasing one-photon detectors. Moreover, quantum double-well potential is formed at the point of ground state splitting providing necessary condition for quantum bits and quantum detectors. To summarize, Josephson φ -junctions can be realized using up-to-date technology and may become important basic element in superconducting electronics.

Acknowledgments

We gratefully acknowledge V. V. Ryazanov helpful discussions. This work was supported by the Russian Foundation for Basic Research (Grants 12-02-90010-Bel-a, 11-02-12065-ofi-m), Russian Ministry of Education and Science, Dynasty Foundation and Dutch FOM.

Appendix A: Ramp type junctions. Limit of small L .

In the limit of small spacing between S electrodes

$$L \ll \min\{\xi_F, \xi_N\} \quad (\text{A1})$$

we can neglect nongradient terms in (4)

$$\frac{\partial}{\partial x} \left(G_{F,N}^2 \frac{\partial}{\partial x} R_{F,N} \right) + \frac{\partial}{\partial z} \left(G_{F,N}^2 \frac{\partial}{\partial z} R_{F,N} \right) = 0, \quad (\text{A2})$$

$$\frac{\partial}{\partial x} \left(G_{F,N}^2 \frac{\partial}{\partial x} U_{F,N} \right) + \frac{\partial}{\partial z} \left(G_{F,N}^2 \frac{\partial}{\partial z} U_{F,N} \right) = 0, \quad (\text{A3})$$

and introduce four functions

$$\Phi_F = R_F + iU_F, \quad \Phi_N = R_N + iU_N, \quad (\text{A4})$$

where, i , is imaginary unit, R_F and R_N are even function of coordinate x , while U_F and U_N are odd in x . Due to the symmetry at $x = 0$

$$\frac{\partial R_{F,N}}{\partial x} = 0, \quad U_{F,N} = 0 \quad (\text{A5})$$

for any coordinate z , and it is convenient to rewrite boundary conditions (9a), (9b) at $x = L/2$ in the form

$$\gamma_{BN} \xi_N \frac{\partial R_N}{\partial x} = \frac{G_S}{G_N} (\Delta \cos(\varphi/2) - R_N), \quad (\text{A6a})$$

$$\gamma_{BF} \xi_F \frac{\partial R_F}{\partial x} = \frac{G_S}{G_F} \left(\frac{\tilde{\omega}}{\omega} \Delta \cos(\varphi/2) - R_F \right), \quad (\text{A6b})$$

$$\gamma_{BN} \xi_N \frac{\partial U_N}{\partial x} = \frac{G_S}{G_N} (\Delta \sin(\varphi/2) - U_N), \quad (\text{A7a})$$

$$\gamma_{BF} \xi_F \frac{\partial U_F}{\partial x} = \frac{G_S}{G_F} \left(\frac{\tilde{\omega}}{\omega} \Delta \sin(\varphi/2) - U_F \right). \quad (\text{A7b})$$

At NF interface the boundary conditions transforms to:

$$\gamma_{BFN} \xi_F \frac{\partial R_F}{\partial z} = -\frac{G_N}{G_F} \left(R_F - \frac{\tilde{\omega}}{\omega} R_N \right), \quad (\text{A8a})$$

$$\gamma_{BNF} \xi_N \frac{\partial R_N}{\partial z} = \frac{G_F}{G_N} \left(R_N - \frac{\omega}{\tilde{\omega}} R_F \right), \quad (\text{A8b})$$

$$\gamma_{BFN} \xi_F \frac{\partial U_F}{\partial z} = -\frac{G_N}{G_F} \left(U_F - \frac{\tilde{\omega}}{\omega} U_N \right), \quad (\text{A9a})$$

$$\gamma_{BNF} \xi_N \frac{\partial U_N}{\partial z} = \frac{G_F}{G_N} \left(U_N - \frac{\omega}{\tilde{\omega}} U_F \right). \quad (\text{A9b})$$

From (A5) and (A6a) - (A7b) it follows that for γ_{BF} and γ_{BN} within the interval

$$\frac{L}{\xi_N} \ll \gamma_{BN} \ll \frac{\xi_N}{L}, \quad \frac{L}{\xi_1} \ll \gamma_{BF} \ll \frac{\xi_1}{L}, \quad (\text{A10})$$

we can neglect $U_{N,F}$ in left hand side of (A7a), (A7b). Moreover, in this approximation for any point inside the weak link region $R_{F,N} \gg U_{F,N}$ and the boundary problem (A2)-(A9b) for functions R_F and R_N can be solved resulting in

$$R_N = \Delta \cos(\varphi/2), \quad R_F = \frac{\tilde{\omega}}{\omega} \Delta \cos(\varphi/2) \quad (\text{A11})$$

and

$$G_N = G_F = \frac{\omega}{\sqrt{\omega^2 + \Delta^2 \cos^2(\varphi/2)}} \quad (\text{A12})$$

Therefore under conditions (A10) both G_N and G_F are independent on coordinate x, z functions and equations for $U_{F,N}$ transform to Laplas equations, which have the solutions

$$U_N = \frac{\Delta \sin(\varphi/2)}{\gamma_{BN}} \frac{G_S}{G_N} \frac{x}{\xi_N} + \sum_{n=1}^{\infty} a_n \sin \frac{\pi(2n+1)x}{L} \cosh \frac{\pi(2n+1)(z-d_N-d_F)}{L}, \quad (\text{A13})$$

$$U_F = \frac{\Delta \sin(\varphi/2)}{\gamma_{BF}} \frac{\tilde{\omega}}{\omega} \frac{G_S}{G_F} \frac{x}{\xi_F} + \frac{\tilde{\omega}}{\omega} \sum_{n=1}^{\infty} b_n \sin \frac{(2n+1)\pi x}{L} \cosh \frac{\pi(2n+1)z}{L}. \quad (\text{A14})$$

They automatically satisfy the boundary conditions at $z = 0$ and $z = d_N + d_F$, as well as at $x = 0$ and $x = L/2$. To find the integration constants a_n and b_n we have to substitute (A13) and (A14) into (A9a), (A9b) and get

$$a_n = -\frac{\Delta \sin(\varphi/2) G_S \Theta \gamma_{BFN} \xi_F t_n}{G_N \beta \cosh \frac{\pi(2n+1)d_N}{L}}, \quad t_n = \tanh \frac{\pi(2n+1)d_N}{L}, \quad (\text{A15})$$

$$b_n = \frac{\Delta \sin(\varphi/2) G_S \Theta \gamma_{BNF} \xi_N t_f}{G_N \beta \cosh \frac{\pi(2n+1)d_F}{L}}, \quad t_f = \tanh \frac{\pi(2n+1)d_F}{L},$$

where

$$\beta = \left(\gamma_{BNF} \xi_N \frac{\pi(2n+1)}{L} t_n + 1 \right) \gamma_{BFN} \xi_F t_f + \gamma_{BNF} \xi_N t_n,$$

and

$$\Theta = \left(\frac{1}{\gamma_{BN}\xi_N} - \frac{1}{\gamma_{BF}\xi_F} \right) \frac{4L}{\pi^2} \frac{(-1)^n}{(2n+1)^2}.$$

Substitution of (A13) and (A14) into expression for the supercurrent (5) gives that contributions to the supercurrent across the junction proportional to a_n and b_n cancel each other and $I_S(\varphi)$ equals to the sum

$$I_S(\varphi) = I_N(\varphi) + I_F(\varphi),$$

$$\frac{2eI_N(\varphi)}{\pi TW d_N} = \frac{1}{\gamma_{BN}\xi_N\rho_N} \sum_{\omega=-\infty}^{\infty} \frac{\Delta^2 G_N G_S \sin(\varphi)}{\omega^2}, \quad (\text{A16})$$

$$\frac{2eI_F(\varphi)}{\pi TW d_F} = \frac{1}{\gamma_{BF}\xi_F\rho_F} \sum_{\omega=-\infty}^{\infty} \frac{\Delta^2 G_F G_S \sin(\varphi)}{\omega^2} \quad (\text{A17})$$

of the currents, $I_N(\varphi)$, and, $I_F(\varphi)$, flowing independently across F and N parts of the weak link.

Appendix B: Ramp type junctions. Limit of intermediate L .

For intermediate values of spacing between the S electrodes

$$\xi_1 \ll L \ll \xi_N. \quad (\text{B1})$$

and suppression parameters at SN and SF interfaces belonging to the interval (3) the boundary problem (4)-(9b) can be also solved analytically for sufficiently large suppression parameter γ_{BFN} . Under these restrictions in the first approximation we can neglect the suppression of superconductivity in the N film due to proximity with the F layer and use expressions (A11) and (A14) with $a_n = 0$ as the solution in the N part of the weak link.

To find R_F and U_F we have to solve the linear equations

$$\xi_F^2 \frac{\partial^2}{\partial x^2} R_F + \xi_F^2 \frac{\partial^2}{\partial z^2} R_F - \tilde{\Omega} R_F = 0, \quad (\text{B2})$$

$$\xi_F^2 \frac{\partial^2}{\partial x^2} U_F + \xi_F^2 \frac{\partial^2}{\partial z^2} U_F - \tilde{\Omega} U_F = 0, \quad (\text{B3})$$

with the boundary conditions

$$\gamma_{BF}\xi_F \frac{\partial R_F}{\partial x} = G_S \frac{\tilde{\Omega}}{\Omega} \Delta \cos(\varphi/2), \quad (\text{B4})$$

$$\gamma_{BF}\xi_F \frac{\partial U_F}{\partial x} = G_S \frac{\tilde{\Omega}}{\Omega} \Delta \sin(\varphi/2), \quad (\text{B5})$$

at $x = L/2$, $0 \leq z \leq d_F$ and

$$\gamma_{BFN}\xi_F \frac{\partial R_F}{\partial z} = \frac{\tilde{\Omega}}{\Omega} G_N R_N, \quad (\text{B6})$$

$$\gamma_{BFN}\xi_F \frac{\partial U_F}{\partial z} = \frac{\tilde{\Omega}}{\Omega} G_N U_N, \quad (\text{B7})$$

at $z = d_F$, $0 \leq x \leq L/2$; ($\Omega = \omega/\pi T_C$, $\tilde{\Omega} = \tilde{\omega} \text{sign}(\omega)/\pi T_C$). The boundary problem (B2)-(B7) must be closed by the conditions (7) and (A5) at free interface of the F film and at the line of junction symmetry, respectively.

Spatial distribution of even in coordinate x part of $\Phi_F(x, z)$ can be found in the form of superposition of superconducting correlations induced into F film from superconductors and from the N part of weak link

$$R_F = \frac{\sqrt{\tilde{\Omega}} G_S \Delta \cos(\varphi/2)}{\Omega \gamma_{BF}} \frac{\cosh\left(\sqrt{\tilde{\Omega}} \frac{x}{\xi_F}\right)}{\sinh\left(\sqrt{\tilde{\Omega}} \frac{L}{2\xi_F}\right)} + \frac{\sqrt{\tilde{\Omega}} G_N \Delta \cos(\varphi/2)}{\Omega \gamma_{BFN}} \frac{\cosh\left(\sqrt{\tilde{\Omega}} \frac{x}{\xi_F}\right)}{\sinh\left(\sqrt{\tilde{\Omega}} \frac{d_F}{\xi_F}\right)}. \quad (\text{B8})$$

Solution for the odd part of $\Phi_F(x, z)$ consists of three terms

$$U_F = \frac{\sqrt{\tilde{\Omega}} G_S \Delta \sin(\varphi/2)}{\Omega \gamma_{BN} \gamma_{BFN}} \frac{x \cosh\left(\sqrt{\tilde{\Omega}} \frac{x}{\xi_F}\right)}{\xi_N \sinh\left(\sqrt{\tilde{\Omega}} \frac{d_F}{\xi_F}\right)} - \frac{\tilde{\Omega}^{3/2} G_S \Delta \sin(\varphi/2) \xi_F^2}{\Omega \gamma_{BN} \xi_N \gamma_{BFN} d_F} \sum_{n=-\infty}^{\infty} \frac{(-1)^n \cos\left(\frac{\pi n x}{d_F}\right) \sinh\left(\kappa_n \frac{x}{\xi_F}\right)}{\kappa_n^3 \cosh\left(\kappa_n \frac{L}{2\xi_F}\right)} + \frac{\sqrt{\tilde{\Omega}} G_S \Delta \sin(\varphi/2)}{\Omega \gamma_{BF}} \frac{\sinh\left(\sqrt{\tilde{\Omega}} \frac{x}{\xi_F}\right)}{\cosh\left(\sqrt{\tilde{\Omega}} \frac{L}{2\xi_F}\right)}, \quad (\text{B9})$$

where $\kappa_n^2 = \tilde{\Omega} + (\pi n \xi_F / d_F)^2$. The first two give the part of U_F induced from the N film, while the last has the well known for SFS junction form^{2,3,4}.

From (B8) and (B9) it follows that $R_{-\omega, F}^* = R_{\omega, F}$ and $U_{-\omega, F}^* = U_{\omega, F}$. Substitution of (B8) and (B9) into expression for the supercurrent (5) gives that the $I_S(\varphi)$ dependence is consists of three terms

$$I_S(\varphi) = I_N(\varphi) + I_F(\varphi) + I_{FN}(\varphi). \quad (\text{B10})$$

The first is the supercurrent across the N layer. In considered approximation it coincides with the expression given by (A16). The second term in (B10) is the supercurrent across SFS double barrier structure in the limit of small transparencies of SF interfaces^{69,70}

$$\frac{2eI_F(\varphi)}{\pi TW d_F} = \frac{\Delta^2 \sin(\varphi)}{\gamma_{BF}^2 \xi_F \rho_F} \sum_{\omega=-\infty}^{\infty} \frac{G_S^2}{\omega^2 \sqrt{\tilde{\Omega}} \sinh(2q_L)} \quad (\text{B11})$$

and the last consists of two terms, $I_{FN}(\varphi) = I_1(\varphi) + I_2(\varphi)$ having different φ -dependence

$$\frac{2eI_1(\varphi)}{\pi TW d_F} = \frac{\Delta^2 \sin(\varphi)}{\rho_F d_F} \frac{\xi_F}{\gamma_{BF} \gamma_{BFN} \gamma_{BN} \xi_N} \sum_{\omega=-\infty}^{\infty} \frac{G_S^2}{\Omega^2 \omega^2} \Psi_1, \quad (\text{B12})$$

$$\Psi_1 = \frac{\sqrt{\tilde{\Omega}}}{\sinh(q_L)} - \frac{2\tilde{\Omega}}{\sinh(2q_L)},$$

$$\frac{2eI_2(\varphi)}{\pi TW d_F} = \frac{\Delta^2 \sin(\varphi)}{\gamma_{BFN} \rho_F d_F} \sum_{\omega=-\infty}^{\infty} \frac{G_N G_S}{\omega^2 \Omega^2} \left(\frac{1}{\gamma_{BN} \gamma_{BFN} \xi_N} \Psi_2 + \frac{\tilde{\Omega}}{\gamma_{BF} \cosh q_L} \right),$$

$$\Psi_2 = \frac{d_F \tilde{\Omega} (2q_d + \sinh(2q_d))}{4q_d \sinh^2(q_d)} - \frac{\tilde{\Omega} \xi_F}{q_d \cosh(q_L)} - \sum_{n=1}^{\infty} \frac{2\tilde{\Omega}^3 \xi_F}{q_d \kappa_n^4 \cosh\left(\frac{L \kappa_n}{2\xi_F}\right)}, \quad (\text{B13})$$

where $q_d = d_F \sqrt{\tilde{\Omega}}/\xi_F$, $q_L = L \sqrt{\tilde{\Omega}}/2\xi_F$. In real experimental situation

$$\xi_F \ll \xi_N, d_F \gg \xi_F. \quad (\text{B14})$$

Under the conditions (B14) some terms of $I_{FN}(\varphi)$ can be neglected. Still existing expressions of it parts $I_{FN1}(\varphi) - I_{FN3}(\varphi)$ simplify to

$$\frac{2eI_{FN1}(\varphi)}{\pi T W d_F} = \frac{\Delta^2 \sin(\varphi)}{\gamma_{BF} \gamma_{BFN} \gamma_{BN} \rho_F d_F} \frac{\xi_F}{\xi_N} \sum_{\omega=-\infty}^{\infty} \frac{G_S^2}{\omega^2 \tilde{\Omega}^2} \frac{\sqrt{\tilde{\Omega}}}{\sinh q_L}, \quad (\text{B15})$$

$$\frac{2eI_{FN2}(\varphi)}{\pi T W d_F} = \frac{\Delta^2 \sin(\varphi)}{2\gamma_{BN} \gamma_{BFN}^2 \rho_F d_F} \sum_{\omega=-\infty}^{\infty} \frac{G_N G_S}{\omega^2 \tilde{\Omega}^{3/2}} \frac{\xi_F}{\xi_N}, \quad (\text{B16})$$

$$\frac{2eI_{FN3}(\varphi)}{\pi T W d_F} = \frac{\Delta^2 \sin(\varphi)}{\gamma_{BFN} \gamma_{BF} \rho_F d_F} \sum_{\omega=-\infty}^{\infty} \frac{G_N G_S}{\omega^2 \tilde{\Omega}} \frac{1}{\cosh q_L}, \quad (\text{B17})$$

Appendix C: Overlap SN-N-NS junctions.

To calculate critical current of SN-N-NS junctions we consider the most practical case of thin N film

$$d_N \ll \xi_N \quad (\text{C1})$$

and sufficiently large γ_{BFN} providing the absence of suppression of superconductivity in N film due to proximity with F layer. We will also assume that electrode spacing L is also small

$$L \ll \xi_N, \quad (\text{C2})$$

in order to have nonsinusoidal CPR.

Condition (C1) permits to perform averaging of Usadel equations in z -direction in N film, as it was described in detail in⁴⁴, and reduce the problem to the solution of one dimensional equations for $\Phi_N = R_N + iU_N$. The real part of Φ_N is the solution of the boundary problem

$$\frac{\xi_N^2 \gamma_{BM}}{G_N (\Omega \gamma_{BM} + G_S)} \frac{\partial}{\partial x} \left(G_N^2 \frac{\partial R_N}{\partial x} \right) - R_N = -r \Delta \cos \frac{\varphi}{2}, \quad \frac{L}{2} \leq x \leq \infty, \quad (\text{C3})$$

$$\frac{\xi_N^2}{\Omega G_N} \frac{\partial}{\partial x} \left(G_N^2 \frac{\partial R_N}{\partial x} \right) = 0, \quad 0 \leq x \leq \frac{L}{2}, \quad (\text{C4})$$

$$\frac{\partial R_N}{\partial x} = 0, \quad x = 0, \quad x \rightarrow \infty, \quad (\text{C5})$$

where $r = G_S/(\Omega \gamma_{BM} + G_S)$, $\gamma_{BM} = \gamma_{BN} d_N/\xi_N$, $\delta = \Delta/\pi T_C$.

From (C4), (C5) it follows that at $0 \leq x \leq L/2$ functions R_N are independent on x constants resulting in

$$\frac{\partial R_N}{\partial x} \left(\frac{L}{2} \right) = 0. \quad (\text{C6})$$

The arising boundary problem (C3), (C5), (C6) is also satisfied by independent on x constants leading to

$$R_N = r \Delta \cos(\varphi/2), \quad 0 \leq x < \infty. \quad (\text{C7})$$

Introducing now new functions, θ

$$U_N = \mu \tan \theta, \quad G_N = \frac{\Omega}{\mu} \cos \theta, \quad (\text{C8})$$

where $\mu = \sqrt{\Omega^2 + r^2 \delta^2 \cos^2(\varphi/2)}$, we get

$$\lambda^2 \frac{\partial^2}{\partial x^2} \theta - \sin(\theta - \phi) = 0, \quad \frac{L}{2} \leq x < \infty, \quad (\text{C9})$$

$$\frac{\xi_N^2}{\cos \theta} \frac{\partial^2}{\partial x^2} \theta = 0, \quad 0 \leq x \leq \frac{L}{2}, \quad (\text{C10})$$

$$\theta(0) = 0, \quad \frac{\partial \theta}{\partial x} = 0, \quad x \rightarrow \infty, \quad (\text{C11})$$

where

$$\lambda = \xi_N \sqrt{\frac{\Omega \gamma_{BM}}{(\Omega \gamma_{BM} + G_S) \sqrt{\Omega^2 + r^2 \delta^2}}}, \quad (\text{C12})$$

$$\tan \phi = \frac{r \sin(\varphi/2)}{\mu}. \quad (\text{C13})$$

Solution of Eq. (C10) can be easily found

$$\theta(x) = \frac{2x}{L} \theta\left(\frac{L}{2}\right), \quad 0 \leq x \leq \frac{L}{2}. \quad (\text{C14})$$

Solution of Eq. (C9) can be simplified due to existence of the first integral

$$\frac{\lambda^2}{2} \left(\frac{\partial}{\partial x} \theta \right)^2 + \cos(\theta - \phi) = 1. \quad (\text{C15})$$

The constant of integration in the right hand side of (C15) have been found from the boundary condition (C11), which demands $\theta \rightarrow \phi$ then $x \rightarrow \infty$. Further integration in (C15) for $L/2 \leq x < \infty$ gives

$$\theta = \phi + 4 \arctan \left(C_2 \exp \left(-\frac{x - L/2}{\lambda} \right) \right), \quad (\text{C16})$$

where C_2 is integration constant, which should be determined from the matching conditions at $x = L/2$. For C_2 they give

$$(\phi + 4 \arctan(C_2)) = -\frac{2C_2}{1 + C_2^2} \frac{L}{\lambda}. \quad (\text{C17})$$

Assuming additionally that γ_{BM} is not too small, namely that $L \ll \xi_N \min(1, \sqrt{\gamma_{BM}})$, from (C17) it is easy to get

$$C_2 = -\tan \left(\frac{\phi}{4} - \frac{L}{4\lambda} \sin \frac{\phi}{2} \right), \quad (\text{C18})$$

resulting in

$$\theta(x) = \frac{2x}{\lambda} \sin \frac{\phi}{2}, \quad 0 \leq x \leq \frac{L}{2}. \quad (\text{C19})$$

From (C19) it follows that in weak link region $|x| \leq L/2$

$$U_N = \frac{2x}{\lambda} \mu \sin \frac{\phi}{2}, \quad G_N = \frac{\Omega}{\mu}, \quad (\text{C20})$$

while under the S electrode, $L/2 \leq x < \infty$

$$U_N = \mu \tan(\phi - 4 \arctan(u)), \quad u = \tan\left(\frac{\phi}{4} - \frac{L}{4\lambda} \sin \frac{\phi}{2}\right) \exp\left(-\frac{x-L/2}{\lambda}\right). \quad (\text{C21})$$

Substitution of (C7), (C20) into expression (5) for the supercurrent in the N channel results in

$$\frac{2eI_N(\phi)}{\pi T W d_N} = \frac{2}{\rho_N \xi_N \sqrt{\gamma_{BM}}} \sum_{\omega=-\infty}^{\infty} \frac{r^2 \delta^2 \sin \phi \sqrt{(\Omega \gamma_{BM} + G_S)}}{\sqrt{2\Omega \mu^2 (\sqrt{\Omega^2 + r^2 \delta^2} + \mu)}}. \quad (\text{C22})$$

Appendix D: Solution in Ferromagnet Layer of RTO junction.

Spatial distribution of even and odd in coordinate x parts of $\Phi_F(x, z)$ can be found in the form of superposition of superconducting correlations induced into F film from superconductors and from the N part of weak link. It has the same form as in (B8) and (B9)

$$R_F = \frac{\sqrt{\Omega} G_S \Delta \cos(\phi/2)}{\Omega \gamma_{BF}} \frac{\cosh\left(\sqrt{\Omega} \frac{x}{\xi_F}\right)}{\sinh\left(\sqrt{\Omega} \frac{L}{2\xi_F}\right)} + \frac{\sqrt{\Omega} G_N R_N}{\Omega \gamma_{BFN}} \frac{\cosh\left(\sqrt{\Omega} \frac{x}{\xi_F}\right)}{\sinh\left(\sqrt{\Omega} \frac{d_F}{\xi_F}\right)}, \quad (\text{D1})$$

$$U_F = \frac{\sqrt{\Omega} G_N U_N}{\Omega \gamma_{BFN}} \frac{\cosh\left(\sqrt{\Omega} \frac{x}{\xi_F}\right)}{\sinh\left(\sqrt{\Omega} \frac{d_F}{\xi_F}\right)} - \frac{\tilde{\Omega}^{3/2} \xi_F^2 G_N (U_N/x)}{\Omega \gamma_{BFN} d_F} \sum_{n=-\infty}^{\infty} \frac{(-1)^n \cos\left(\frac{n\pi x}{d_F}\right) \sinh\left(\kappa_n \frac{x}{\xi_F}\right)}{\kappa_n^3 \cosh\left(\kappa_n \frac{L}{2\xi_F}\right)} + \frac{\sqrt{\Omega} G_S \delta \sin(\phi/2)}{\Omega \gamma_{BF}} \frac{\sinh\left(\sqrt{\Omega} \frac{x}{\xi_F}\right)}{\cosh\left(\sqrt{\Omega} \frac{L}{2\xi_F}\right)}, \quad (\text{D2})$$

with the functions R_N , G_N , and U_N defined by equations followed from the solution of the boundary problem in the N layer described in Appendix C.

$$R_N = r \Delta \cos(\phi/2), \quad G_N = \frac{\Omega}{\sqrt{\Omega^2 + r^2 \delta^2 \cos^2(\phi/2)}}, \quad (\text{D3})$$

$$U_N = \alpha \Delta \sin(\phi/2) \frac{G_S}{G_N} \frac{x}{\xi_N}, \quad \alpha = \frac{2\sqrt{\Omega^2 + \delta^2}}{\sqrt{2(\sqrt{\Omega^2 + r^2 \delta^2} + \mu)}} \frac{r}{\sqrt{1-r}}. \quad (\text{D4})$$

Substitution of (D1)-(D4) into expression (5) gives that supercurrent across F layer in RTO junction consists of the sum of $I_F(\phi)$ and $I_{FN}(\phi)$, where $I_F(\phi)$ is the current through one dimensional double barrier SFS structure defined by Eq. (B11), while $I_{FN}(\phi) = I_1(\phi) + I_2(\phi)$ has the form

$$\frac{2eI_1(\phi)}{\pi T W d_F} = \frac{\Delta^2 \sin(\phi)}{\rho_F d_F} \frac{\xi_F}{\gamma_{BF} \gamma_{BFN} \xi_N} \sum_{\omega=-\infty}^{\infty} \frac{\alpha G_S^2}{\Omega^2 \omega^2} \Psi_1, \quad \Psi_1 = \frac{\sqrt{\tilde{\Omega}}}{\sinh(qL)} - \frac{2\tilde{\Omega}}{\sinh(2qL)}, \quad (\text{D5})$$

$$\frac{2eI_2(\phi)}{\pi T W d_F} = \frac{\Delta^2 \sin(\phi)}{\rho_F d_F} \frac{1}{\gamma_{BFN}} \sum_{\omega=-\infty}^{\infty} \frac{r G_N G_S}{\omega^2 \Omega^2} \left(\frac{\alpha}{\gamma_{BFN} \xi_N} \Psi_2 + \frac{\tilde{\Omega}}{\gamma_{BF} \cosh qL} \right), \quad \Psi_2 = \frac{d_F \tilde{\Omega} (2q_d + \sinh(2q_d))}{4q_d \sinh^2(q_d)} - \frac{\tilde{\Omega} \xi_F}{q_d \cosh(qL)} - \sum_{n=1}^{\infty} \frac{2\tilde{\Omega}^3 \xi_F}{q_d \kappa_n^4 \cosh\left(\frac{L \kappa_n}{2\xi_F}\right)}. \quad (\text{D6})$$

Application of conditions (B14) allows to neglect some terms in $I_{FN}(\phi) = I_{FN1}(\phi) + I_{FN2}(\phi) + I_{FN3}(\phi)$ and to simplify remaining terms, leading to the following expressions:

$$\frac{2eI_{FN1}(\phi)}{\pi T W d_F} = \frac{\Delta^2 \sin(\phi)}{\gamma_{BF} \gamma_{BFN} \rho_F d_F} \frac{\xi_F}{\xi_N} \sum_{\omega=-\infty}^{\infty} \frac{\alpha G_S^2}{\omega^2 \Omega^2} \frac{\sqrt{\tilde{\Omega}}}{\sinh qL}, \quad (\text{D7})$$

$$\frac{2eI_{FN2}(\phi)}{\pi T W d_F} = \frac{\Delta^2 \sin(\phi)}{2\gamma_{BFN}^2 \rho_F d_F} \sum_{\omega=-\infty}^{\infty} \frac{r \alpha G_N G_S}{\omega^2 \tilde{\Omega}^{3/2}} \frac{\xi_F}{\xi_N}, \quad (\text{D8})$$

$$\frac{2eI_{FN3}(\phi)}{\pi T W d_F} = \frac{\Delta^2 \sin(\phi)}{\gamma_{BFN} \gamma_{BF} \rho_F d_F} \sum_{\omega=-\infty}^{\infty} \frac{r G_N G_S}{\omega^2 \tilde{\Omega}} \frac{1}{\cosh qL}. \quad (\text{D9})$$

- ¹ K.K. Likharev, Rev. Mod. Phys. **51**, 1079 (1979).
- ² A. A. Golubov, M. Yu. Kupriyanov, E. Il'ichev, Rev. Mod. Phys. **76**, 411 (2004).
- ³ A. I. Buzdin, Rev. Mod. Phys. **77**, 935 (2005).
- ⁴ F. S. Bergeret, A. F. Volkov, K. B. Efetov, Rev. Mod. Phys. **77**, 1321 (2005).
- ⁵ V. V. Ryazanov, V. A. Oboznov, A. Yu. Rusanov, A. V. Veretenikov, A. A. Golubov, and J. Aarts, Phys. Rev. Lett. **86**, 2427 (2001).
- ⁶ S. M. Frolov, D. J. Van Harlingen, V. A. Oboznov, V. V. Bolginov,

- and V. V. Ryazanov, Phys. Rev. B **70**, 144505 (2004);
- ⁷ T. Kontos, M. Aprili, J. Lesueur, F. Genet, B. Stephanidis, and R. Boursier, Phys. Rev. Lett. **89**, 137007 (2002).
- ⁸ H. Sellier, C. Baraduc, F. Lefloch, and R. Calemczuck, Phys. Rev. B **68**, 054531 (2003).
- ⁹ Y. Blum, A. Tsukernik, M. Karpovskii, and A. Palevski, Phys. Rev. B **70**, 214501 (2004).
- ¹⁰ C. Surgers, T. Hoss, C. Schonenberger, C. Strunk, J. Magn. Magn. Mater. **240**, 598 (2002).
- ¹¹ C. Bell, R. Loloee, G. Burnell, and M. G. Blamire Phys. Rev. B

- 71**, 180501 (R) (2005).
- 12 S. M. Frolov, D. J. Van Harlingen, V. V. Bolginov, V. A. Oboznov, and V. V. Ryazanov, *Phys. Rev. B* **74**, 020503 (2006).
- 13 V. A. Oboznov, V. V. Bol'ginov, A. K. Feofanov, V. V. Ryazanov, and A. I. Buzdin, *Phys. Rev. Lett.* **96**, 197003 (2006).
- 14 V. Shelukhin, A. Tsukernik, M. Karpovski, Y. Blum, K. B. Efetov, A. F. Volkov, T. Champel, M. Eschrig, T. Lofwander, G. Schon, and A. Palevski, *Physical Review B* **73**, 174506 (2006).
- 15 M. Weides, K. Tillmann, and H. Kohlstedt, *Physica C* **437-438**, 349 (2006).
- 16 M. Weides, M. Kemmler, H. Kohlstedt, A. Buzdin, E. Goldobin, D. Koelle, R. Kleiner, *Appl. Phys. Lett.* **89**, 122511 (2006).
- 17 M. Weides, M. Kemmler, H. Kohlstedt, R. Waser, D. Koelle, R. Kleiner, and E. Goldobin *Physical Review Letters* **97** 247001 (2006).
- 18 J. Pfeiffer, M. Kemmler, D. Koelle, R. Kleiner, E. Goldobin, M. Weides, A. K. Feofanov, J. Lisenfeld, and A. V. Ustinov, *Physical Review B* **77**, 214506 (2008).
- 19 H. Sellier, C. Baraduc, F. Lefloch, and R. Calemczuck, *Phys. Rev. Lett.* **92**, 257005 (2004).
- 20 F. Born, M. Siegel, E. K. Hollmann, H. Braak, A. A. Golubov, D. Yu. Gusakova, and M. Yu. Kupriyanov, *Phys. Rev. B.* **74**, 140501 (2006).
- 21 J. W. A. Robinson, S. Piano, G. Burnell, C. Bell, and M. G. Blamire, *Phys. Rev. Lett.* **97**, 177003 (2006).
- 22 S. Piano, J. W.A. Robinson, G. Burnell, M. G. Blamire *The European Physical Journal B* **58**, 123 (2007).
- 23 J. W. Robinson, S. Piano, G. Burnell, C. Bell, and M. G. Blamire *Physical Review B* **76**, 094522 (2007).
- 24 R. S. Keizer, S. T. B. Goennenwein, T. M. Klapwijk, G. Miao, G. Xiao, A. Gupta, *Nature* **439**, 825 (2006).
- 25 T. S. Khaire, M. A. Khasawneh, W. P. Pratt, Jr., and N. O. Birge, *Phys. Rev. Lett.* **104**, 137002 (2010).
- 26 J. W. A. Robinson, J. D. S. Witt, and M. G. Blamire, *Science* **329**, 59 (2010).
- 27 J. Wang, M. Singh, M. Tian, N. Kumar, B. Liu, C. Shi, J. K. Jain, N. Samarth, T. E. Mallouk and M. H. W. Chan, *Nat. Phys.* **6**, 389 (2010).
- 28 M. S. Anwar, F. Czeschka, M. Hesselberth, M. Porcu, and J. Aarts, *Phys. Rev. B* **82**, 100501(R) (2010).
- 29 M. S. Anwar, M. Veldhorst, A. Brinkman, and J. Aarts, *Appl. Phys. Lett.* **100**, 052602 (2012).
- 30 T. Ortlev, Ariando, O. Mielke, C. J. M. Verwijs, K. F. K. Foo, H. Rogalla, F. H. Uhlmann, and H. Hilgenkamp, *Science* **312**, 1495 (2006).
- 31 A.K. Feofanov, V.A. Oboznov, V.V. Bol'ginov, *et. al.*, *Nature Physics* **6**, 593 (2010).
- 32 A. V. Ustinov and V. K. Kaplunenko, *J. Appl. Phys.* **94**, 5405 (2003).
- 33 R.G. Mints, *Phys. Rev. B* **57**, R3221 (1998).
- 34 A. Buzdin and A. E. Koshelev, *Phys. Rev. B* **67**, 220504(R) (2003).
- 35 N. G. Pugach, E. Goldobin, R. Kleiner, and D. Koelle, *Phys. Rev. B* **81**, 104513 (2010).
- 36 M. Yu. Kupriyanov, A.A. Golubov, M. Siegel, *Proceedings of the SPIE*, **6260**, 62600S-1 (2006).
- 37 E. Goldobin, D. Koelle, R. Kleiner, and R.G. Mints, *Phys. Rev. Lett.* **107**, 227001 (2011); H. Sickinger, A. Lipman, M Weides, R.G. Mints, H. Kohlstedt, D. Koelle, R. Kleiner, and E. Goldobin, *arXiv* 1207.3013.
- 38 E. Goldobin, D. Koelle, R. Kleiner, and A. Buzdin, *Phys. Rev. B*, **76**, 224523 (2007).
- 39 N. V. Klenov, N. G. Pugach, A. V. Sharafiev, S. V. Bakurskiy, V. K. Kornev, *Physics of Solid State*, **52**, 2246 (2010).
- 40 A. S. Vasenko, A. A. Golubov, M. Yu. Kupriyanov, and M. Weides, *Phys. Rev. B*, **77** 134507 (2008).
- 41 A. S. Vasenko, S. Kawabata, A. A. Golubov, M. Yu. Kupriyanov, C. Lacroix, F. W. J. Hekking, *Phys. Rev. B* **84** 024524 (2011).
- 42 F. Konschelle, J. Cayssol, A.I. Buzdin, *Phys. Rev. B* **78**, 134505 (2008).
- 43 M. Houzet, V. Vinokur, and F. Pistolesi, *PRB* **72**, 220506 (2005)
- 44 T. Yu. Karminskaya and M. Yu. Kupriyanov, *Pis'ma Zh. Eksp. Teor. Fiz.* **85**, 343 (2007) [*JETP Lett.* **85**, 286 (2007)].
- 45 T. Yu. Karminskaya and M. Yu. Kupriyanov, *Pis'ma Zh. Eksp. Teor. Fiz.* **85**, 343 (2007) [*JETP Lett.* **86**, 61 (2007)].
- 46 T. Yu. Karminskaya, M. Yu. Kupriyanov, and A. A. Golubov, *Pis'ma Zh. Eksp. Teor. Fiz.* **87**, 657 (2008) [*JETP Lett.*, **87**, 570 (2008)].
- 47 Karminskaya T. Yu., Golubov A. A., Kupriyanov M. Yu., Sidorenko A. S., *Phys. Rev. B* **79**, 214509 (2009).
- 48 T. Yu. Karminskaya, A. A. Golubov, M. Yu. Kupriyanov, and A. S. Sidorenko *Phys. Rev. B* **81**, 214518 (2010).
- 49 S. V. Bakurskiy, N. V. Klenov, T. Yu. Karminskaya, M. Yu. Kupriyanov and V. K. Kornev, *Solid State Phenomena*, **190**, 401 (2012).
- 50 F. S. Bergeret, A. F. Volkov, and K. B. Efetov, *Phys. Rev. Lett.* **86**, 3140 (2001).
- 51 Ya. V. Fominov, N. M. Chtchelkatchev, and A. A. Golubov, *Phys. Rev. B* **66**, 014507 (2002).
- 52 A. Furusaki and M. Tsukada, *Solid State Commun.* **78**, 299 (1991).
- 53 A. Furusaki and M. Tsukada, *Phys. Rev. B* **43**, 10 164 (1991).
- 54 Z. G. Ivanov, M. Yu. Kupriyanov, K. K. Likharev, S. V. Meriakri, and O. V. Snigirev, *Fiz. Nizk. Temp.* **7**, 560 (1981). [*Sov. J. Low Temp. Phys.* **7**, 274 (1981)]
- 55 A. A. Zubkov, and M. Yu. Kupriyanov, *Fiz. Nizk. Temp.* **9**, 548 (1983) [*Sov. J. Low Temp. Phys.* **9**, 279 (1983)].
- 56 M. Yu. Kupriyanov, *Pis'ma Zh. Eksp. Teor. Fiz.* **56**, 414 (1992). [*JETP Lett.* **56**, 399 (1992)].
- 57 Demler, E. A., Arnold G. B., and Beasley M. R., *Phys. Rev. B* **55**, 15174 (1997).
- 58 K. D. Usadel, *Phys. Rev. Lett.* **25**, 507 (1970).
- 59 M. Yu. Kupriyanov and V. F. Lukichev, *Sov. Phys. JETP* **67**, 1163 (1988) [*Zh. Eksp. Teor. Fiz.* **94**, 139 (1988)].
- 60 N. M. Chtchelkatchev and I. S. Burmistrov, *Phys. Rev. B* **68**, 140501(R) (2003).
- 61 I. S. Burmistrov and N. M. Chtchelkatchev, *Phys. Rev. B* **72**, 144520 (2005).
- 62 T. Champel and M. Eschrig, *PRB* **72**, 054523 (2005).
- 63 M. Houzet and A. I. Buzdin, *Phys. Rev. B* **74**, 214507 (2006).
- 64 M. A. Maleki and M. Zareyan *Physical Review B* **74**, 144512 (2006).
- 65 Y. V. Fominov, A. F. Volkov, and K. B. Efetov, *Phys. Rev. B* **75**, 104509 (2007).
- 66 A. F. Volkov and A. Anishchanka, *Phys. Rev. B* **71**, 024501 (2005).
- 67 A. F. Volkov, K. B. Efetov *Phys Rev B* **78**, 024519 (2008).
- 68 B. Crouzy, S. Tollis, D. A. Ivanov, *Phys. Rev. B* **76**, 134502 (2007).
- 69 A. A. Golubov, M. Yu. Kupriyanov, and Ya. V. Fominov, *JETP Lett.* **75**, 709 (2002) [*Pisma v ZhETF* **75**, 588 (2002)].
- 70 A. Buzdin, *JETP Lett.* **78**, 1073 (2003) [*Pisma v ZhETF* **78**, 1073 (2003)].
- 71 M. Yu. Kupriyanov, V. F. Lukichev, A. A. Orlikovskii, *Mikroelektronika* **15**, 328 (1986) [*Soviet Microelectronics* **15**, 185 (1986)].